October 1, 1992

Development of a Fast RICH Detector with a Solid Cesium-Iodide Photocathode: Summary of Research in FY92

N. S. Lockyer and J. E. Millan
Department of Physics, David Rittenhouse Laboratories
University of Pennsylvania, Philadelphia, PA, 19104

C. Lu and K. T. McDonald
Joseph Henry Laboratories, Princeton University,
Princeton, NJ 08544

A. Lopez
Department of Physics
University of Puerto Rico, Mayaguez, Puerto Rico, 00708

D. F. Anderson and S. Kwan
Fermi National Accelerator Laboratory, Batavia, IL 60510

Abstract

We have studied the performance of solid CsI photocathodes and achieved quantum efficiencies of nearly 35% at 190 nm in small test chambers. The paper reporting these results have been accepted for publication in Nuclear Instruments and Methods (N.I.M.). We also built and tested a prototype, low-pressure parallel-plate Čerenkov detector, at Brookhaven and have submitted a paper to N.I.M. reporting the observation of Čerenkov rings.

Contents

List of Figures

1 Progress at Fermilab

During the past year, significant progress has been made on understanding the basic properties of the CsI and CsI-TMAE photocathodes [1]. The activities have concentrated on the systematic study of various factors which would affect the quantum efficiency and aging characteristics of the photocathode.

Two major factors have been found which would improve the quantum efficiency of the photocathode by a factor of 3 or more. These are heating of the photocathode during preparation, and the gas environment when operating the photocathodes. The quantum efficiency obtained is about 35% for pure CsI at 170 nm and about 45% for CsI-TMAE. This results agrees with the group at CERN which obtained the result by flowing the gas.

The dependence of the photocathode aging on the operating temperature, on the presence of gas, on the gas gain, and the presence of TMAE as well as the incoming light flux have been studied in detail. For CsI photocathodes, charges in excess of 2×10^{14} e^-/mm^2 can be collected with little degradation of performance of the photocathode. This result means that the CsI photocathode will survive at the SSC.

Recently, studies have been done on making a photocathode by spraying a solution of CsI in distilled water directly on the substrate. The quantum efficiency is about 30% lower.

A summary of this work is presented in the attached Fermilab preprint along with a plot of the performance of the sprayed-on photocathode. Based on this work, we believe these photocathodes are now ready for use in high energy physics experiments.

2 Progress at U. Penn

The principal activity last year was perfecting the design and building the prototype low-pressure, parallel-plate Čerenkov detector. In addition, we fabricated three different types of printed circuit boards. These boards are used to mount the readout electronics, including the SVX chips.

A significant effort was made in learning to make large area photocathodes. We achieved about 30% of the quantum efficiency achieved in the smaller test chamber at Princeton and Fermilab. These studies are continuing, but the materials involved in the construction are of maybe outgassing and the vacuum system is of poorer quality than in the test systems.

A beam test was performed at both Fermilab, January 1991, and at Brookhaven during the summer of 1992. The results are summarized in an attached paper [2], written jointly with our Princeton collaborators. The principal result is that we were able to observe Čerenkov rings.

3 Progress at Princeton University

In addition to participation in the construction and testing of the prototype RICH detector described above, we have made a number of benchtop studies of photocathodes, gas mixtures, and radiators. The equipment for these studies was funded in part by the Texas National Research Laboratory Commission, and by matching funds from Princeton University.

3.1 Monte Carlo simulation of the RICH detector

To understand the various factors of the efficiency of the prototype RICH detector a simple Monte Carlo program has been written. Here we present some details discussed only briefly in ref. [2]

The following physical processes were included in the simulation:

1. The Čerenkov-light spectrum per unit length of radiator and unit wavelength interval is:
$$\frac{d^2N}{d\lambda dL} = 2\pi\alpha\frac{\sin^2\theta_C}{\lambda^2} = 4.58\times 10^5\frac{\sin^2\theta_C}{\lambda^2},$$
where λ is in nm, and the radiator length L is in cm.

2. The index of refraction of the C_6F_{14} liquid radiator as a function of wavelength was taken as follows [3]:
$$n_{C_6F_{14}}(E) = 1.2733 + 9.3\times 10^{-3}(E-6),$$
where photon energy E is in eV. The Čerenkov angle for index 1.273 is 38°.

3. The wavelength interval for photon detection was taken as 170-220 nm, so the average number $\bar{N}$ of Čerenkov photons per cm of radiator in this interval is
$$\bar{N} = 462.62\sin^2\theta_C = 179.37.$$

4. The actual number N of photons was Gaussian distributed with average $\bar{N}$ and $\sigma = \sqrt{\bar{N}}$, and were randomly distributed along the track of a minimum-ionizing particle in the radiator.

5. The external transmission of C_6F_{14} was measured with a Perkin-Elmer Lambda 3 spectrophotometer within a region of 190-220 nm, and corrected for the reflection at the interfaces air-to-UV-window and liquid-to-UV-window to obtain the internal transmission. Due to the lack of a VUV spectrophotometer we were not able to measure the transmission for 170-190 nm. For $\lambda < 190$ nm we used data from Arnold *et al.* [3], who report that the transmission of C_6F_{14} is not sensitive to the purification procedure in this region. The data points with a fitting curve are shown in Fig. 1. The apparatus we used to purify the C_6F_{14} is shown in Fig. 2.

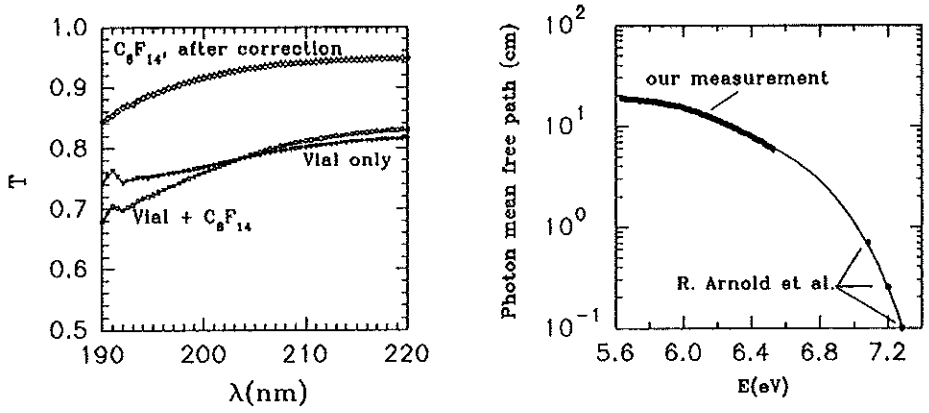

Figure 1: a) Spectrophotometer scans of transmission of C_6F_{14} liquid in a 1-cm-pathlength vial. b) The mean free path for uv light in C_6F_{14} as a function of photon energy. The three data points at high energy are from Arnold *et al.* [3].

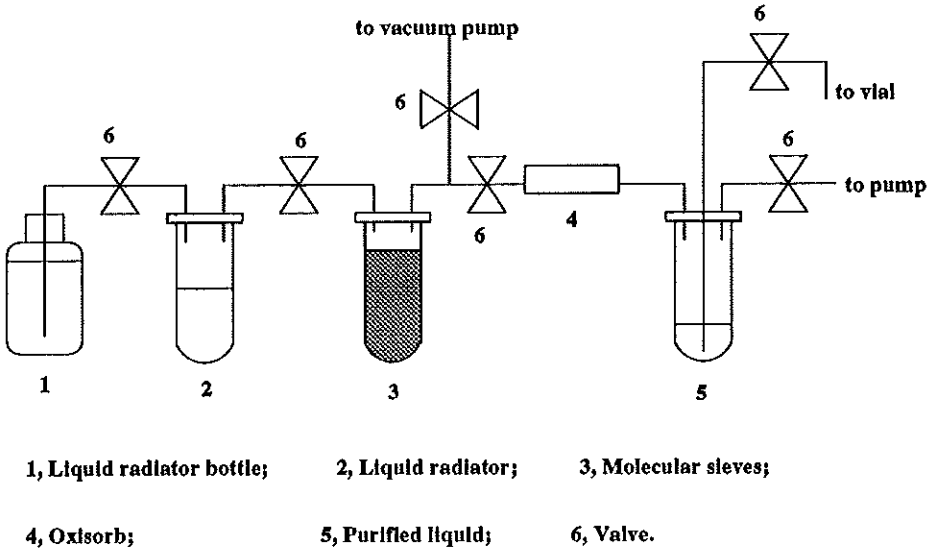

Figure 2: Sketch of the apparatus used to purify liquid C_6F_{14}. The Oxisorb is the most important purification stage.

6. The refractive index of UV-grade fused silica was taken from the Melles-Griot catalog as:

$$n_Q^2 - 1 = \frac{0.6961663\lambda^2}{\lambda^2 - (0.0684043)^2} + \frac{0.4079426\lambda^2}{\lambda^2 - (0.1162414)^2} + \frac{0.8974794\lambda^2}{\lambda^2 - (9.896161)^2},$$

for λ in μm. A typical value is $n_Q = 1.57$ at 190 nm.

7. The internal transmission of the UV-grade fused silica window was taken from the Melles-Griot catalog. The mean free path length μ *vs.* wavelength was taken as

$$\mu = \frac{1}{\ln(1 - 10^{3.07223 - 0.023856\lambda})},$$

with λ in nm.

8. The reflection of Čerenkov light on the interfaces between fused silica and air is governed by Fresnel's equations. Because the Čerenkov radiation is linearly polarized in the plane of incidence (containing the direction of observation and the path of the particle), the coefficient of reflection is

$$R_{\|} = \left[\frac{n_t \cos\theta_i - n_i \cos\theta_t}{n_t \cos\theta_i + n_i \cos\theta_t}\right]^2.$$

The angles of Čerenkov light in vacuum, quartz and the C_6F_{14} radiator are related by

$$\sin\theta = n_Q \sin\theta_Q = n_{C_6F_{14}} \sin\theta_C, \qquad \text{so that} \qquad \theta \approx 52^\circ \qquad \text{and} \qquad \theta_Q \approx 30^\circ.$$

For both the vacuum-quartz and quartz-liquid interfaces we are very near the Brewster angle at which $R_{\|}$ vanishes.

9. The transmittance of the anode mesh was considered as a constant. For normal incidence the transmittance was $(0.9)^2 = 0.81$, the square of the ratio of the spacing between wires to the spacing of wire centers. Čerenkov light is incident on the mesh at 52° from the normal, so the transmission factor in each projection $(L' - a)/L'$ varies between 0.9 and 0.83 as illustrated in Fig. 3. The combined transmission varies between $(0.9)(0.83) = 0.75$ and $(0.83)^2 = 0.69$, and we take 0.72 as the average transmittance.

10. The quantum efficiency of the CsI photocathode was inferred from work of Anderson *et al.* [1], who report results with both methane and isobutane chamber gas. Our gas, ethane, is expected to have performance intermediate between these two gases, so we calculate for both methane and isobutane.

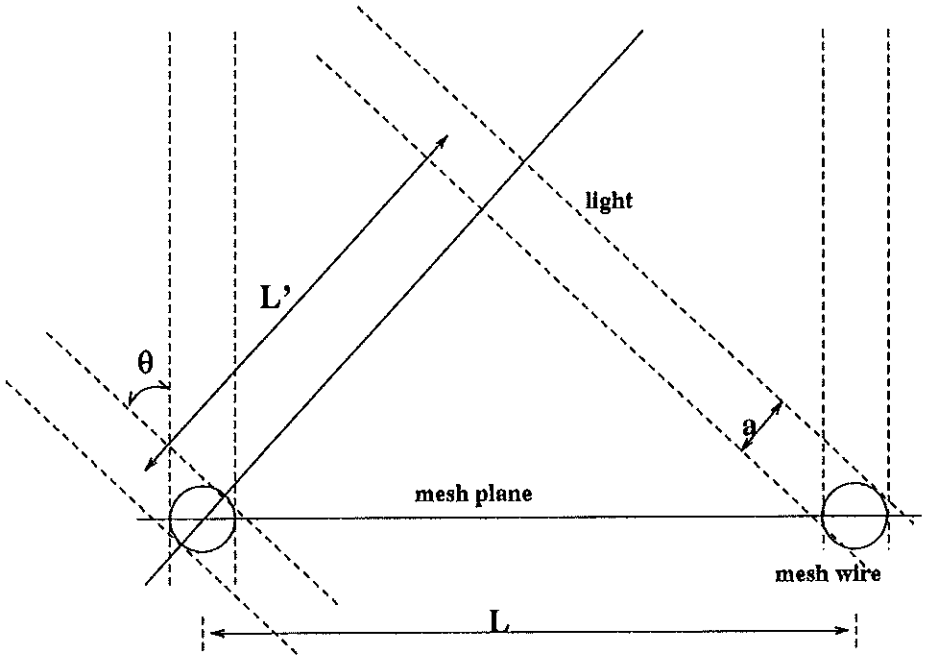

Figure 3: Transmittance of a mesh to Čerenkov light.

11. For each photoelectron ejected from the photocathode, a Townsend avalanche was generated according to Polya distribution [4] for the observed gas gain g:

$$P(g) = \left(\frac{b}{b-1}\frac{g}{\bar{g}}\right)^{b-1} e^{(b-1-bg/\bar{g})},$$

where $\bar{g}$ is the mean gas gain, and b is a measure of the fluctuation in gain. We took $\bar{g} = 10^5$, and $b = 1.5$ in our calculation. The threshold of the electronics was set at $g = 2000$.

The simulation of the RICH detector was carried out for methane and isobutane chamber gas and for four different radiator lengths from 1 to 4 cm. The various efficiency distributions used in our simulation are shown in Fig. 4. The total number of detected photons are shown in Fig. 5. For data collected at BNL with the RICH prototype we used a 2-cm-thick radiator. If we suppose ethane gas is close to isobutane in performance with a CsI photocathode, the expected number of hits per Čerenkov ring would be 20.

3.2 Measurement of quantum efficiency of CSI cathodes

At Princeton U. we have built a small facility to fabricate and test CsI photocathodes. The cathodes are evaporated in a Denton DV-502 vacuum evaporator equipped with

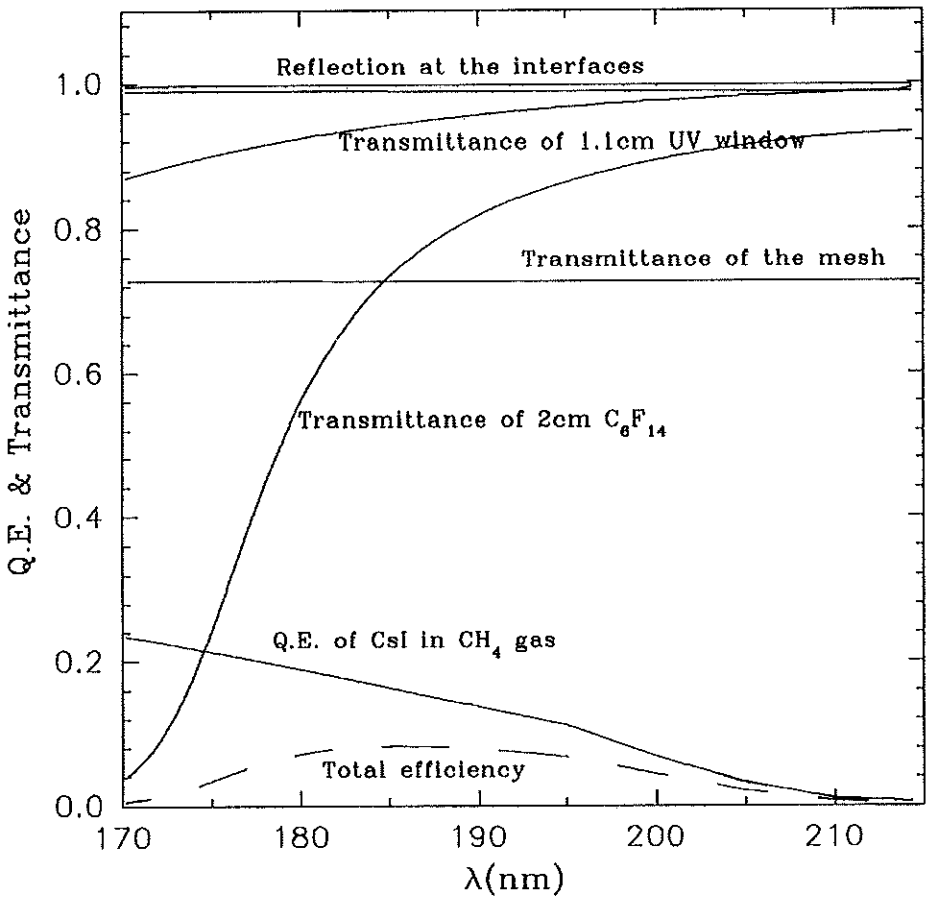

Figure 4: Various efficiency distributions that enter the simulation.

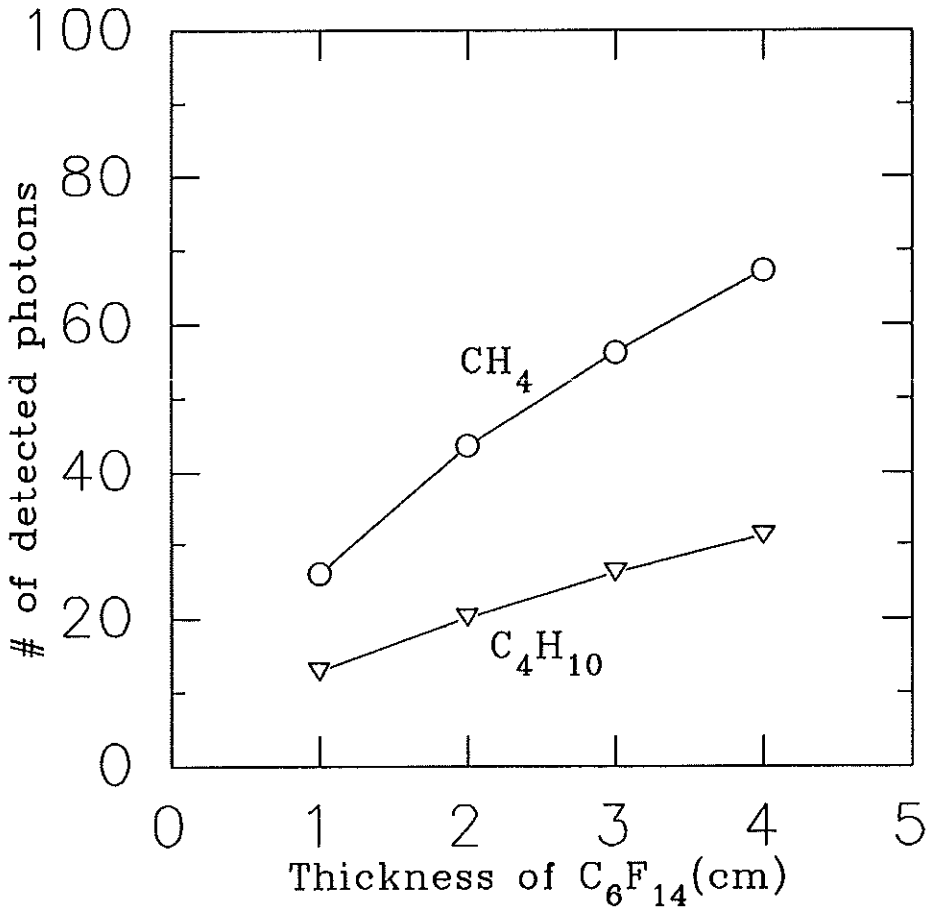

Figure 5: Prediction of the total number of detected photons in our RICH prototype if the photocathode had the quantum efficiency reported by Anderson *et al.* [1].

a Balzers TPD020 molecular drag pump and oil-free diaphragm pump. The cathode substrate can be heated during evaporation by water piped in from a circulating temperature bath and/or by infrared lamp shining through the glass bell jar.

The quantum efficiency of the cathodes can be evaluated in a small test chamber shown in Fig. 6. UV light is derived from a pulsed hydrogen lamp (Hamamatsu) and the desired wavelength selected with a monochromator (Instruments SA model H1061). For studies down to 170-nm wavelength, the cutoff of uv-grade quartz, all light paths must be in nitrogen. The photocathode is mounted in a small parallel-plate chamber patterned after the work of Hoeneisen *et al.* [5], which permits use of TMAE photosensitive gas as the reference for quantum efficiency.

Only recently, and after considerable effort, have we produced photocathodes that meet (and exceed) the high quantum efficiencies reported by Anderson *et al.* [1]. Very exacting standards of care and cleanliness must be maintained during the fabrication procedure. Our best cathodes are made from pure CsI obtained in crystal form from Bicron Co. Figure 7 shows our measured quantum efficiency *vs.* wavelength for a cathode used with isobutane gas at various pressures.

Studies of cathodes used with methane and ethane are in progress.

Older studies with a low-quantum-efficiency cathode permitted measurements of the optical transmission of methane, ethane and isobutane at wavelengths below 190 nm, at which our commercial spectrophotometer does not operate (due to absorption by oxygen in the air). Figure 8 shows the transmission of uv light through the 2.5-cm-thick gas-filled chamber gap. This is not an absolute measurement, but shows that isobutane is much less transparent than ethane or methane below 175 nm.

As the quartz cutoff is 170 nm, the maximum quantum efficiency in a RICH detector could be obtained with methane of ethane gas rather than isobutane – provided the radiator is also transparent at down to 170 nm. From Figure 1 we see that liquid C_6F_{14} does not satisfy this criterion. In the future we will investigate the use of C_8F_{18} as the radiator, since the vendor (3M Fluorinert Products, type FC-104) advises us this liquid is more transparent in the uv. A vacuum spectrophotometer will be required for these studies.

We have also studied the possibility of operating the CsI photocathode RICH detectors at atmospheric pressure. This would greatly ease the difficulty of construction of large-scale detectors. However, as demonstrated by Anderson [6] several years ago, a gas at atmospheric pressure reflects about 50% of the photoelectrons back onto the photocathode where they are lost. We have verified this for helium/methane and helium/ethane gas mixtures, as shown in Figs. 9 and 10. Nonetheless, a RICH detector with the high quantum efficiency of Fig. 5 has enough photoelectrons that atmospheric-pressure operation may be viable.

The use of helium as the buffer gas retains the desirable feature that the detector is largely blind to minimum-ionizing particles.

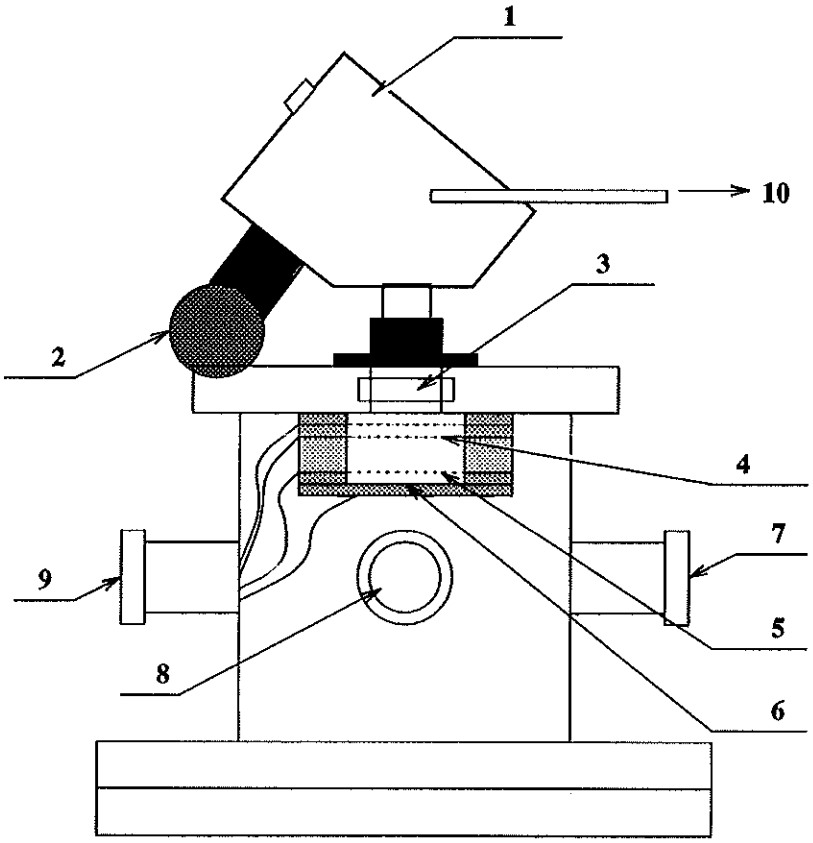

1, Monochromator; **2, Hydrogen lamp;** **3, UV window;**
4, Mesh; **5, Anode mesh;** **6, Photocathode;**
7, Vacuum port; **8, Gas port;** **9, Signal & H.V. port;**
10, To Nitrogen gas botttle.

Figure 6: The test chamber for measurement of quantum efficiency *vs.* wavelength.

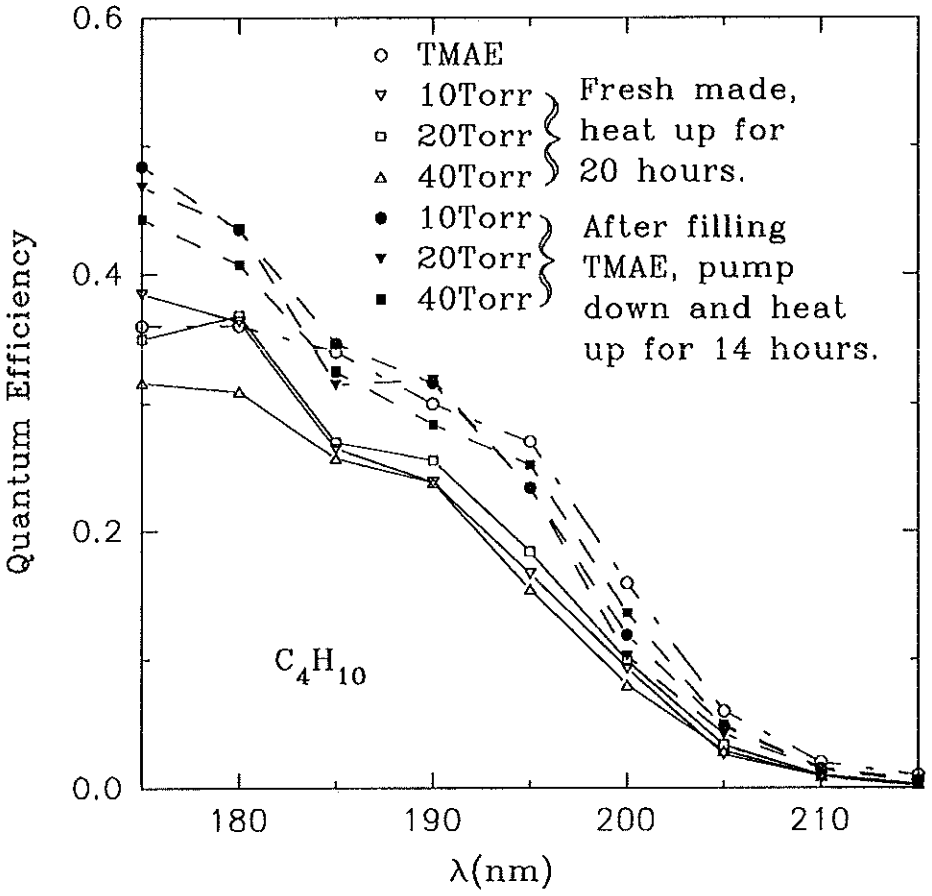

Figure 7: The quantum efficiency *vs.*wavelength for a CsI photocathode used with isobutane gas at various pressures.

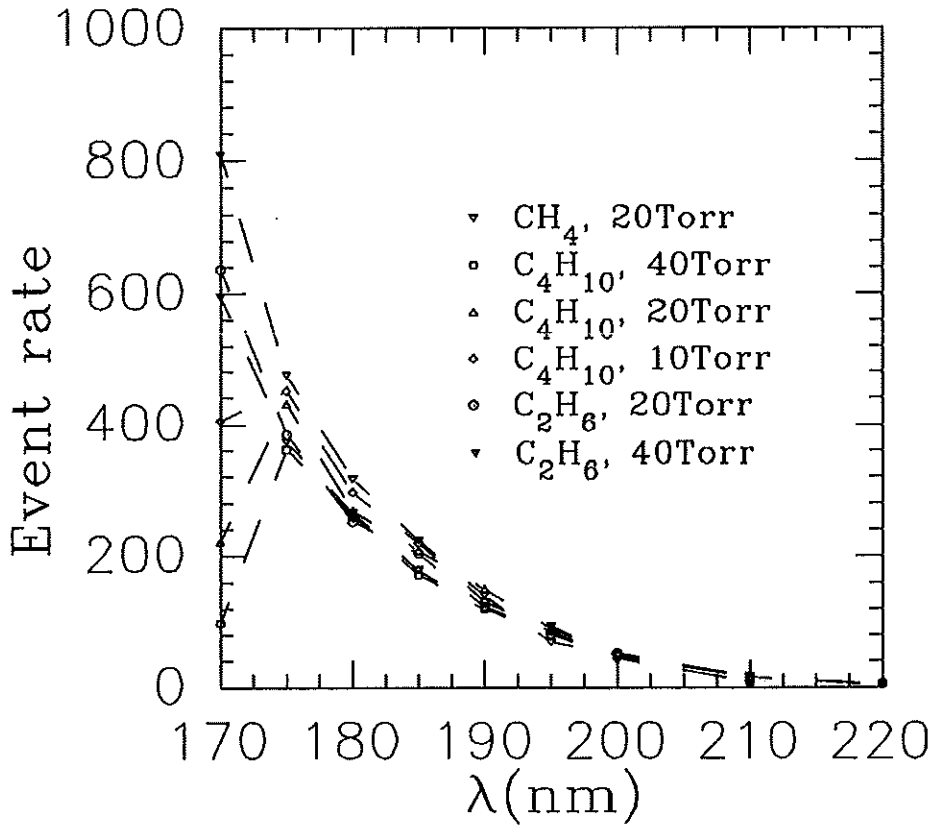

Figure 8: The relative transmission of light in methane, ethane and isobutane *vs.* wavelength. Isobutane is significantly less transparent than methane or ethane for 170-175 nm.

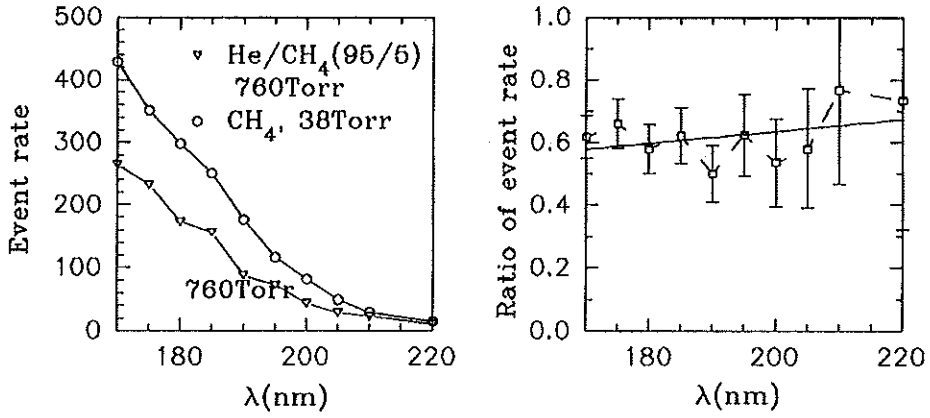

Figure 9: a) The quantum efficiency (unnormalized) of a CsI photocathode used with 38-torr methane and 760-torr He/CH_4 (95/5) *vs.*wavelength. b) The relative quantum efficiency from a), showing that use of atmospheric-pressure helium as a buffer causes a 40% loss of quantum efficiency at all wavelengths.

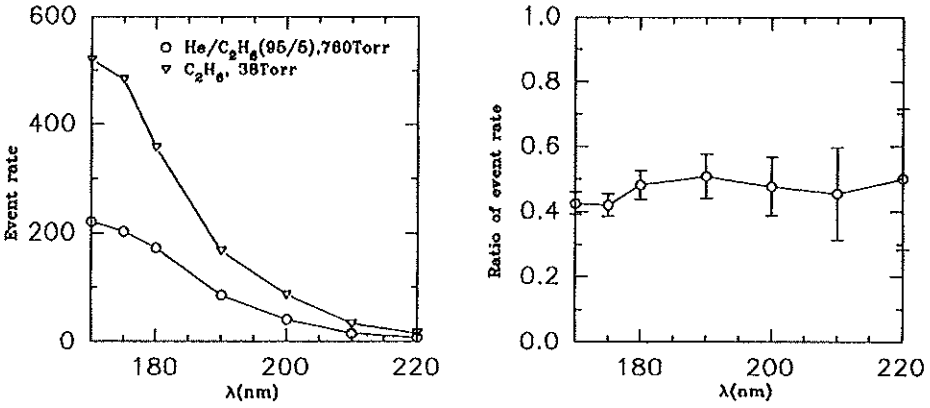

Figure 10: a) The quantum efficiency (unnormalized) of a CsI photocathode used with 38-torr methane and 760-torr He/C_2H_6 (95/5) *vs.*wavelength. b) The relative quantum efficiency from a), showing that use of atmospheric-pressure helium as a buffer causes a 50% loss of quantum efficiency at all wavelengths.

References

[1] D.F. Anderson *et al.*, *Properties of CsI and CsI-TMAE Photocathodes*, FERMILAB-Conf-92/135 (June 1992), Proceedings to be published in Nucl. Instr. and Meth. A.

[2] N.S. Lockyer *et al.*, *Observation of Čerenkov Rings Using a Low-Pressure Parallel-Plate Chamber and a Solid Cesium-Iodide Photocathode*, UPR-0217E, Princeton/HEP/92-08 (Sept. 1992).

[3] R. Arnold *et al.*, *A Ring Imaging Čerenkov Detector, the Delphi Barrel RICH Prototype*, Nucl. Instr. and Meth. **A270** (1988) 289.

[4] J. Byrne, *Statistics of the Electron Multiplication Process in Proportional Counters.* Proc. Roy. Soc. Edin. **66A** (1962) 33.

[5] B. Hoeneisen, D. F. Anderson and S. Kwan, *A CsI-TMAE Photocathode with Low-Pressure Readout for RICH*, Nucl. Instr. and Meth. **A302** (1991) 447.

[6] D.F. Anderson *et al.*, *coupling of a BaF_2 Scintillator to a TMAE Photocathode and a Low-Pressure Wire Chamber*, Nucl. Instr. and Meth. **217** (1983) 217.